Biochimica et Biophysica Acta xxx (2013) xxx–xxx

Contents lists available at SciVerse ScienceDirect

Biochimica et Biophysica Acta

journal homepage: www.elsevier.com/locate/bbagen

Multi-target-directed design, syntheses, and characterization of fluorescent bisphosphonate derivatives as multifunctional enzyme inhibitors in mevalonate pathway

Q1 Jinbo Gao [b], Jinggong Liu [a], Yongge Qiu [b], Xiusheng Chu [b], Yuqin Qiao [b], Ding Li [a,*]

[a] School of Pharmaceutical Sciences, Sun Yat-sen University, Guangzhou University City, 132 Waihuan East Road, Guangzhou 510006, PR China
[b] Department of Biology and Chemistry, City University of Hong Kong, 83 Tat Chee Avenue, Kowloon, Hong Kong, PR China

ARTICLE INFO

Article history:
Received 13 December 2012
Received in revised form 30 January 2013
Accepted 12 February 2013
Available online xxxx

Keywords:
Bisphosphonate
Multifunctional inhibitor
Mevalonate kinase
Phosphomevalonate kinase
Mevalonate 5-diphosphate decarboxylase
Farnesyl pyrophosphate synthase

ABSTRACT

Background: Mevalonate pathway is an important cellular metabolic pathway present in all higher eukaryotes and many bacteria. Four enzymes in mevalonate pathway, including MVK, PMK, MDD, and FPPS, play important regulatory roles in cholesterol biosynthesis and cell proliferation. Q2

Methods: The following methods were used: cloning, expression and purification of enzymes in mevalonate pathway, organic syntheses of multifunctional enzyme inhibitors, measurement of their IC_{50} values for above four enzymes, kinetic studies of enzyme inhibitions, molecular modeling studies, cell viability tests, and fluorescence microscopy.

Results and conclusions: We report our multi-target-directed design, syntheses, and characterization of two blue fluorescent bisphosphonate derivatives compounds **15** and **16** as multifunctional enzyme inhibitors in mevalonate pathway. These two compounds had good inhibition to all these four enzymes with their IC_{50} values at nanomolar to micromolar range. Kinetic and molecular modeling studies showed that these two compounds could bind to the active sites of all these four enzymes. The fluorescence microscopy indicated that these two compounds could easily get into cancer cells.

General significance: Multifunctional enzyme inhibitors are generally more effective than single enzyme inhibitors, with fewer side effects. Our results showed that these multifunctional inhibitors could become lead compounds for further development for the treatment of soft-tissue tumors and hypercholesteremia.

1. Introduction

The mevalonate pathway is an important cellular metabolic pathway present in all higher eukaryotes and many bacteria, and has so far been exploited in the design of drugs treating and preventing human diseases, including cardiovascular diseases and osteoporosis [1]. This pathway is also a potentially important target for the treatment of tumors especially bearing mutations in protein p53 [2,3]. Farnesyl pyrophosphate synthase (FPPS) is a key regulatory enzyme in the mevalonate pathway [4]. Besides, mevalonate pathway also contains a unique series of three sequential ATP-dependent enzymes that convert mevalonate to isopentenyl diphosphate (IPP): mevalonate kinase (MVK), phosphomevalonate kinase (PMK), and mevalonate 5-diphosphate decarboxylase (MDD). These three enzymes catalyze consecutive steps downstream from HMG-CoA reductase in the mevalonate pathway, and are responsive to cholesterol in-take in animals. The blockade of the mevalonate pathway is a concept that has found widespread clinical use, with statins as drugs that inhibit HMG-CoA reductase and reduce cholesterol biosynthesis [5], and nitrogen-containing bisphosphonates (*N*-BPs) as drugs for osteoporosis therapy that target FPPS and inhibit protein prenylation [6]. Some multiple inhibitory compounds, including statins [7], bisphosphonates [8], farnesyl transferase inhibitors (FTIs), and geranyl geranyltransferase inhibitors (GGTIs) [9], have been developed previously targeting mevalonate pathway. Statin's side effects have been the subject of much controversy over the past few decades, since more and more research is revealing serious potential adverse reactions from statin medications [10–12].

Bisphosphonate therapy has been considered as standard therapy in the management and care of cancer patients with metastatic bone disease and patients with osteoporosis with fewer side effects [13–15]. In addition, bisphosphonates can be easily modified in various positions of their P-C-P structure. Its central carbon has great metabolic stability, and also provides a scaffold that can be modified

Abbreviations: FPP, farnesyl pyrophosphate; FPPS, farnesyl pyrophosphate synthase; GPP, geranyl diphosphate; HMG-CoA reductase, 3-hydroxy-3-methylglutaryl-CoA reductase; IPP, isopentenyl diphosphate; MDD, mevalonate 5-diphosphate decarboxylase, also known as mevalonate 5-pyrophosphate decarboxylase or MPD; MTT, 3-(4,5-dimethylthiazol-2-yl)-2,5-diphenyl-tetrazolium bromide; MVAPP, mevalonate 5-diphosphate; MVK, mevalonate kinase; *N*-BPs, nitrogen-containing bisphosphonates; PMK, phosphomevalonate kinase; PP, pyrophosphate or diphosphate; TsCl, toluene sulfonyl chloride

* Corresponding author. Tel.: +86 13 5337 65290 fax: +86 20 3994 3058.
E-mail address: liding@mail.sysu.edu.cn (D. Li).

0304-4165/$ – see front matter © 2013 Published by Elsevier B.V.
http://dx.doi.org/10.1016/j.bbagen.2013.02.011

with additional substituents, such as the hydroxyl group and heteroaromatic rings found in risedronate and zoledronate [16,17]. However, these bisphosphonates all bear substantial negative charge at physiological pH, which limit the compounds' ability to penetrate the cell membrane. In an effort to circumvent this perceived limitation, some biodegradable protecting groups have been used to mask a negative charge until after penetration of the cell membrane [18,19]. Further investigation and improvement of bisphosphonates are still required.

Our strategy in the design of novel multifunctional inhibitors based on bisphosphonates is to link some known enzyme inhibitors with covalent chemical bond in the P-C-P backbone, which targets on four different enzymes in the mevalonate pathway, including MVK, PMK, MDD, and FPPS. In the present paper, we report our multi-target-directed design, syntheses, and characterization of two bisphosphonate derivatives as multifunctional enzyme inhibitors in the mevalonate pathway, which mainly contain the following functional groups: the first one is bisphosphonate targeting on FPPS; the second one is geranyl group with aromatic substitution targeting on ATP binding site of MVK, PMK, and MDD; and the third one is mevalonate group with fluorine substitution targeting on mevalonate binding site of MVK, PMK, and MDD.

2. Materials and Methods

2.1. Materials

Lactate dehydrogenase, pyruvate kinase, phosphoenol pyruvate, NADH, (*RS*)-mevalonic acid lactone, and ATP were purchased from Sigma. *Taq* DNA polymerase, HB101 competent cells, and *E. coli* strain BL21(DE3) competent cells came from Invitrogen Life Technologies. Synthesized oligonucleotides were obtained from Tech Dragon Company of Hong Kong. T4 DNA ligase and restriction enzymes came from MBI Fermentas of Germany. All other reagents were of research grade or better and were obtained from commercial sources. The rat liver MVK, MDD, and FPPS were obtained and assayed as previously described [20–22]. Tris buffer was used instead of phosphate buffer in enzyme storage and enzyme assay.

2.2. Cloning, expression, and purification of rat PMK

A rat liver Quick-Clone cDNA library was purchased from Clontech (Palo Alto, CA). Standard cloning technology was used to clone the gene of rat PMK. DNA sequencing of the cloned rat PMK gene was performed, and the inserted gene sequence was identified to be the same as previously deposited in NCBI without any mutation. Established methods were used to prepare rat PMK [20], and the protein was purified to apparent homogeneity as shown in SDS-PAGE in supporting information, which was stored at −80 °C in 50 mM potassium phosphate buffer, pH 7.5, 0.1 mM EDTA, 5% glycerol, and 5 mM β-mercaptoethanol. The activity of the enzyme was assayed spectrophotometrically following the decrease in absorbance at 340 nm as reported previously [23].

2.3. Organic syntheses of blue fluorescent bisphosphonate derivatives

^{1}H, ^{13}C, and ^{31}P NMR spectra were recorded on a Varian Mercury 300 MHz NMR spectrometer at room temperature. Chemical shifts are reported in ppm on the δ scale relative to the internal standard TMS. Flash chromatography was performed in columns of various diameters with silica gel by elution with appropriate solvents. Analytical thin layer chromatography (TLC) was carried out on Merck silica gel 60G254 plates (25 mm), and developed with appropriate solvents, and was visualized either with UV light or by dipping into a staining solution of potassium permanganate and then heating. AG MP-1M 100–200 resin, chloride form was from Bio-Rad. Dowex 50 WX2-100 cation-exchange resin was purchased from Aldrich. All other reagents were of research grade or better, and were obtained from commercial sources. Organic syntheses of bisphosphonate derivatives were shown in Scheme 1.

Synthesis of tetraethyl ethenylidenebisphosphonate (**3**). The compound was synthesized following a reported procedure with minor modification [24]. Paraformaldehyde (10.4 g, 0.35 mol) and diethylamine (5.08 g, 0.069 mol) were combined in 0.2 L of methanol, and the mixture was warmed until clear. Compound **1** (20.0 g, 0.069 mol) was added, and the resulting mixture was heated under reflux for 24 h. Then additional 0.2 L of methanol was added, and the solution was concentrated under vacuum at 35 °C. Toluene (0.1 L) was added, and the solution was again concentrated. This last step was repeated to ensure complete removal of methanol to give the product **2** as a clear liquid. ^{1}H NMR ($CDCl_3$) δ 4.02 (m, 8 H, OCH_2CH_3, $J=7.3$ Hz), 3.63 (overlapping m, 2H, CH_3OCH_2, $J=5.4$ Hz and 15.6 Hz), 3.20 (s, 3H, CH_3O), 2.52 (tt, 1H, PCHP, $J=6.0$ Hz and 24.01 Hz), 1.18 (t, 12H, CH_2CH_3, $J=7.1$ Hz).

p-Toluenesulfonic acid monohydrate (0.50 g) was added, and the mixture was heated under reflux. Methanol was removed from the reaction mixture either by collection in a Dean-Stark trap or by adsorption into 4 Å molecular sieves contained in a Soxhlet extractor. After 14 h, the solution was concentrated. The crude product was diluted with 1 L of chloroform, and washed with water (2×150 mL). The solution was dried over $MgSO_4$ and concentrated to give the product **3**. ^{1}H NMR ($CDCl_3$) δ 6.98 (distorted dd, 2H, $H_2C=$, $J=33.8$ Hz and 37.71 Hz), 4.32–4.00 (m, 8H, OCH_2CH_3), 1.32 (t, 12H, OCH_2CH_3, $J=$ 7.1 Hz). This NMR data is consistent with that reported previously [24].

Synthesis of 2-(3-chloropropyl)-2-methyl-1,3-dioxolane (**4**). A mixture of 5-chloro-2-pentanone (19.6 g, 158 mmol), ethylene glycol (49.7 g, 800 mmol), and *p*-toluenesulfonic acid monohydrate (300 mg, 1.6 mmol) was heated in 500 mL of toluene under reflux with a Dean–Stark trap for 24 h. The mixture was then washed with 10% aq. $NaHCO_3$ solution (3×30 mL), followed by brine (3×30 mL). The organic phase was dried over anhydrous Na_2SO_4. After filtration, the solvent was removed under reduced pressure, and the residual liquid was distilled to give 24 g (92%) of compound **4** as a colorless liquid. ^{1}H NMR (300 MHz, $CDCl_3$) δ 3.95 (4 H, m, OCH_2CH_2O), 3.60 (2 H, t, $J=7.0$ Hz, CH_2Cl), 1.85 (4 H, m, CH_2-CH_2), 1.35 (3 H, s, CH_3).

Synthesis of tetraethyl 5-(2-methyl-1,3-dioxolan-2-yl) pentane-1, 1-diyldiphosphonate (**6**). A titrated solution containing 1.66 mmol of the Grignard reactant of the compound **4** (0.062–2.44 M) in THF was slowly added to a magnetically stirred solution of tetraethyl ethenylidenebisphosphonate **3** (500 mg, 1.66 mmol) in dry THF (10 mL) at −15 °C under Ar. The reaction progress was followed by using TLC, and the reaction was usually complete at the end of the addition. The mixture was warmed to room temperature, and then slowly poured into a saturated solution of NH_4Cl (20 mL). The mixture was extracted with ether (2×20 mL), and the combined organic layers were dried and concentrated under reduced pressure. The crude residue was purified by using flash chromatography with appropriate eluent to give the product **6** as an oil. MS (ESI): m/z 431 $(M+H)^+$.

Synthesis of (*E*)-3,7-dimethyl-octa-2,6-dienyl acetate (**7**). To a mixture of alcohol/phenol/amine (1 mmol) and acetic anhydride (1.2 mmol), $La(NO_3)_3 \cdot 6H_2O$ (10 mol%) was added. After completion of the reaction as monitored by using TLC, water was added to the reaction mixture, and the product was extracted into ethyl acetate (3×20 mL). The combined organic layers were washed with brine and concentrated in vacuum, which was purified by using silica gel column chromatography to afford the acetylated product **7**. ^{1}H NMR (300 MHz, $CDCl_3$) δ 5.32 (br t, 1H), 5.06 (m, 1H), 4.57 (d, 2H, $J=$ 7.5Hz), 2.03 (s, 3H), 2.03–2.09 (m, 4H), 1.68 (s, 3H), 1.66 (s, 3H), 1.58 (s, 3H).

Synthesis of (*2E*, *6E*)-3,7-dimethyl-8-oxoocta-2,6-dienyl acetate (**8**). Geranyl acetate (**7**) (6.84 g, 34.9 mmol) pre-dissolved in 100 mL of 95% ethanol was added dropwise over 40 min to a refluxing solution of SeO_2 (5.8 g, 52 mmol) in 300 mL of 95% ethanol. The mixture was heated

Please cite this article as: J. Gao, et al., Multi-target-directed design, syntheses, and characterization of fluorescent bisphosphonate derivatives as multifunctional enzyme inhibitors in mevalonate pathway, Biochim. Biophys. Acta (2013), http://dx.doi.org/10.1016/j.bbagen.2013.02.011

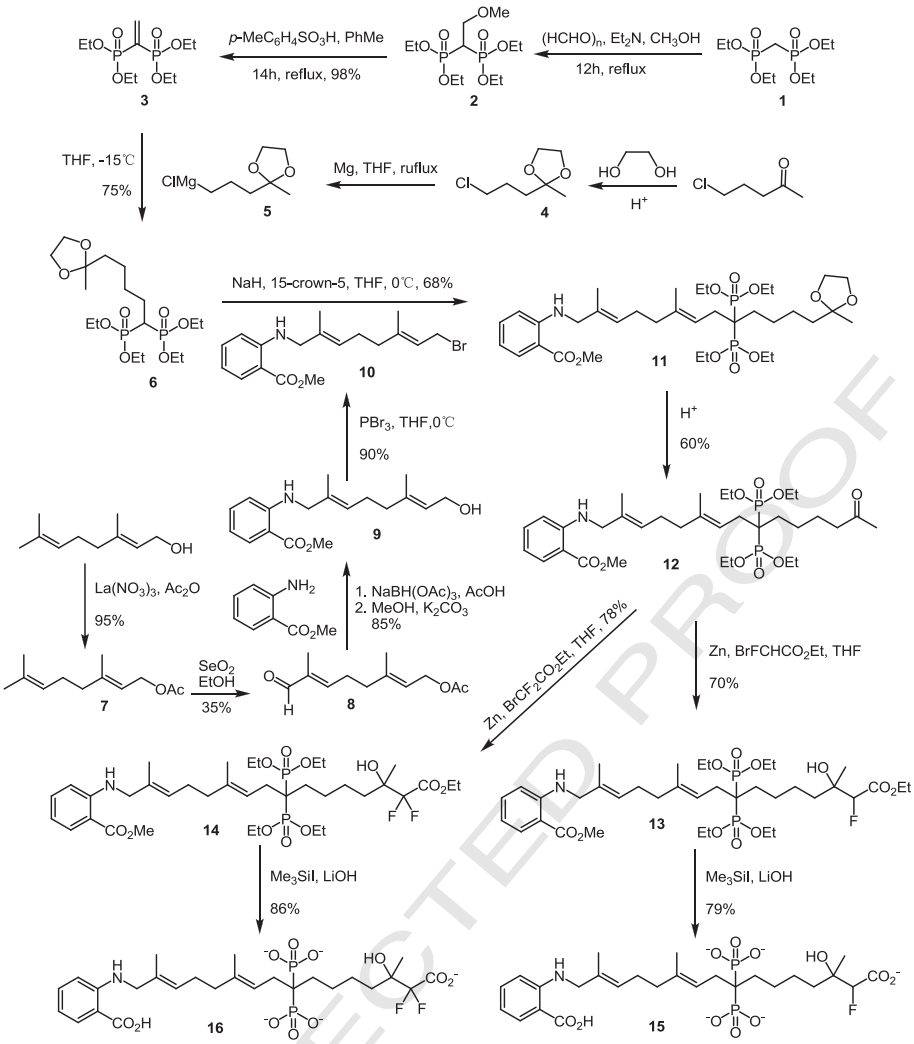

Scheme 1. Organic syntheses of blue fluorescent bisphosphonate derivatives.

under reflux for 22 h. The black precipitate was removed by vacuum filtration over a pad of silica-gel, and washed with 95% ethanol. Solvent was removed at reduced pressure, and 400 mL of ethyl ether was added. Organic layer was washed with brine (4×80 mL), dried over Na_2SO_4, and concentrated under vacuum. The residue was purified by using silica gel column chromatography to give a light yellow oil (2.8 g) with a yield of 41%. R_f 0.75 (7:3 v/v hexanes: EtOAc); ^{1}H NMR (300 MHz, $CDCl_3$) δ 9.37 (s, 1H), 6.46 (d, J=6.0 Hz, 1H), 5.39 (d, J=6.0 Hz, 1H), 4.60 (d, J=7.2 Hz, 2H), 2.50 (q, J=7.5 Hz, 2H), 2.24 (t, J=7.5 Hz, 2H), 2.06 (s, 3H), 1.75 (s, 6H).

Synthesis of methyl 2-((*2E*, *6E*)-8-hydroxy-2,6-dimethyl-octa-2,6-dienylamino) benzoate (**9**). Methyl anthranilate hydrochloride (1.00 g, 5.33 mmol) and aldehyde **8** (4.39 g, 15.5 mmol) were dissolved in $ClCH_2CH_2Cl$ (21 mL). Acetic acid (2.50 mL, 43.2 mmol) and 4 Å molecular sieves were added, and the reaction solution was stirred for 5 min at room temperature. After $NaBH(OAc)_3$ (6.89 g, 32.5 mmol) was added, the solution was stirred for 2.7 h at room temperature, and then quenched by addition of 5% $NaHCO_3$ dropwise at 0 °C. The product was extracted with ether, and the combined extracts were washed with brine, dried with $MgSO_4$, and concentrated to afford a colorless oil. Final purification by using flash column chromatography gave compound **9-OAc** as a colorless oil. K_2CO_3 (7.12 g, 51.6 mmol) was added to **9-OAc** (3.61 g, 17.2 mmol) dissolved in methanol, and the mixture was allowed to stir for 3 h at room temperature. Water was added (300 mL), and methanol was removed at reduced pressure. The aqueous residue was saturated with solid NaCl, and the solution was extracted with ethyl acetate (4×50 mL). The combined organic extracts were dried over $MgSO_4$ and concentrated to give 2.95 g of compound **9** as a yellowish oil. ^{1}H NMR δ 7.89 (d, 1H), 7.82 (br s, 1H), 7.31 (dd, 1H), 6.63 (d, 1H), 6.58 (dd, 1H), 5.42–5.36 (m, 2H), 4.12 (d, 2H, J=7.5 Hz), 3.85 (s, 3H), 3.72 (d, 2H, J=6.5 Hz), 2.22–2.15 (m, 2H), 2.08–2.03 (m, 2H), 1.68 (s, 3H), 1.66 (s, 3H).

Synthesis of methyl 2-((*2E*, *6E*)-8-bromo-2,6-dimethylocta-2,6-dienylamino) benzoate (**10**). The compound was synthesized following a reported procedure with minor modification [25]. To a solution of compound **9** (2.8 g, 12 mmol) in THF at −15 °C were added PBr_3 (15 mmol). The reaction flask was transferred to an ice bath and allowed to stir for 1 h, and then water was added. The mixture was extracted with ether, washed with ice cold brine, dried with $MgSO_4$, and filtered. The solvent was removed in vacuo to give **10** as a yellow oil. ^{1}H NMR δ 7.9 (dd, 1H), 7.32 (ddd, 1H), 6.63 (dd, 1H), 6.59 (ddd, 1H), 5.40 (m, 2H), 4.07 (d, 2H, J=7.0 Hz), 3.83 (s, 3H), 3.74 (d, 2H, J=7.5 Hz), 2.17 (m, 2H), 2.08 (m, 2H), 1.72 (s, 3H), 1.68 (s, 3H). This NMR data is consistent with that reported previously [25].

Synthesis of methyl 2-((*2E*, *6E*)-9,9-bis(diethoxyphosphoryl)-2,6-dimethyl-13-(2-methyl-1,3-dioxolan-2-yl)-trideca-2,6-dienylamino)-benzoate (**11**). To a suspension of NaH (0.94 g, 60% dispersion in mineral oil, 24 mmol) in anhydrous THF at 0 °C was added 15-crown-5 (0.23 mL, 1.2 mmol) followed by compound **6** (5.8 mmol). After 1 h,

Please cite this article as: J. Gao, et al., Multi-target-directed design, syntheses, and characterization of fluorescent bisphosphonate derivatives as multifunctional enzyme inhibitors in mevalonate pathway, Biochim. Biophys. Acta (2013), http://dx.doi.org/10.1016/j.bbagen.2013.02.011

the allylic bromide **10** was added via cannula as a solution in THF. The reaction mixture was allowed to warm to room temperature overnight, and then quenched by addition of water. The mixture was extracted with ether, and the combined organic extracts were dried with $MgSO_4$ and filtered. The filtrate was concentrated in vacuo, and the resulting residue was purified by using flash chromatography to give product **11**. ^{1}H NMR (300 MHz, $CDCl_3$) δ 8.01–7.79 (m, 1H), 7.38–7.25 (t, 1H, J = 7.0 Hz), 6.72–6.51 (q, 2H), 5.51–5.31 (m, 2H), 4.22–3.41 (m, 17H), 2.22–1.21 (m, 35H). MS (ESI): m/z 431 $(M+H)^+$.

Synthesis of methyl 2-((*2E*, *6E*)-9,9-bis-(diethoxyphosphoryl)-2,6-dimethyl-14-oxopentadeca-2,6-dienylamino)-benzoate (**12**). A solution of compound **11** (1.21 mmol) in 80% acetic acid (10 mL) was heated at 65 °C for 1.5 h. The progress of the reaction was followed by TLC (CH_2Cl_2–MeOH, 95:5 v/v). The mixture was cooled to room temperature, and then was concentrated under reduced pressure. The residue was dissolved in CH_2Cl_2 (15 mL), and the resulting solution was washed with a saturated solution of $NaHCO_3$ (4×5 mL), dried and then concentrated under reduced pressure. The crude material was purified by using flash chromatography to give compound **12** as a colorless oil. ^{1}H NMR (300 MHz, $CDCl_3$) δ 7.91–7.81 (m, 1H), 7.41–7.22 (t, 1H), 6.72–6.50 (q, 2H, J = 7.5 Hz), 5.52–5.29 (m, 2H), 4.25–3.75 (m, 13H), 2.46–1.22 (m, 35H).

Synthesis of methyl 2-((*2E*, *6E*)-9,9-bis-(diethoxyphosphoryl)-16-ethoxy-15-fluoro-14-hydroxy-2,6,14-trimethyl-16-oxohexadeca-2,6-dienylamino) benzoate (**13**). To a suspension of zinc dust (1.5 equiv) in THF (0.5 mL/mmol) was added dibromoethane (20 μL/mmol). The mixture was heated under refluxed for a few minutes. A solution of compound **12** (1 equiv.) in THF (1 M) was added dropwise. The reaction was stirred at room temperature for 15 min, and a solution of bromofluoroacetate was added. The reaction mixture was stirred at room temperature for 1.5 h, quenched with saturated solution of NH_4Cl, and extracted with ether. The combined organic layers were washed with saturated aqueous $NaHCO_3$ and saturated aqueous NH_4Cl, and dried with $MgSO_4$. After evaporation of the solvent, the crude product was purified by using flash column chromatography to give compound **13** with a yield of 70%. ^{1}H NMR (300 MHz, $CDCl_3$) δ 7.96–7.82 (m, 1H), 7.39–7.25 (t, 1H, J = 7.5 Hz), 6.75–6.51 (q, 2H, J = 7.2 Hz), 5.51–5.32 (m, 2H), 4.45–3.75 (m, 17H), 2.16–1.25 (m, 38H).

Synthesis of methyl 2-((*2E*, *6E*)-9,9-bis-(diethoxyphosphoryl)-16-ethoxy-15,15-difluoro-14-hydroxyl-2,6,14-trimethyl-16-oxohexadeca-2,6-dienylamino) benzoate (**14**). To a suspension of zinc dust (1.5 equiv.) in THF (0.5 mL/mmol) was added dibromoethane (20 μL/mmol). The mixture was heated under refluxed for a few minutes. A solution of compound **12** (1 equiv.) in THF (1 M) was added dropwise. The reaction was stirred at room temperature for 15 min, and the solution of bromodifluoroacetate was added. The reaction mixture was stirred at room temperature for 1.5 h, quenched with saturated solution of NH_4Cl, and extracted with ether. The combined organic layers were washed with saturated aqueous $NaHCO_3$ and saturated aqueous NH_4Cl, and dried with $MgSO_4$. After evaporation of the solvent, the crude product was purified by using flash column chromatography to give compound **14** with a yield of 78%. ^{1}H NMR (300 MHz, $CDCl_3$) δ 7.96–7.82 (m, 1H), 7.39–7.25 (t, 1H, J = 7.2 Hz), 6.75–6.51 (q, 2H, J = 6.0 Hz), 5.51–5.32 (m, 2H), 4.45–3.75 (m, 16H), 2.16–1.25 (m, 38H).

Synthesis of 2-((*2E*, *6E*)-15-carboxy-15-fluoro-14-hydroxy-2,6,14-trimethyl-9,9-diphosphonopentadeca-2,6-dienylamino) benzoic acid (**15**). To a solution of compound **13** (0.45 mmol) in anhydrous CH_2Cl_2 at 0 °C were added 2,4,6-collidine (0.59 mL, 4.5 mmol) and TMSI (0.58 mL, 4.5 mmol), and the reaction mixture was allowed to warm to room temperature over a period of 2 h. Toluene was then added, and the volatiles were removed in vacuo to afford a white solid. This material was dissolved in aqueous LiOH (5 mL, 1 N) at room temperature. After 24 h, the mixture was lyophilized to afford a gray solid **15**. ^{1}H NMR (300 MHz, D_2O) δ 7.96–7.82 (m, 1H), 7.39–7.25 (t, 1H, J = 7.2 Hz), 6.75–6.51 (q, 2H, J = 7.0 Hz), 5.51–5.32 (m, 2H), 4.45–3.75 (m, 4H), 2.16–1.25 (m, 23H). MS (ESI): m/z 624 $(M+H)^+$. HRMS (m/z): Calcd for $(C_{26}H_{40}FNO_{11}P_2+H)^+$ 624.2133, found 624.2136.

Synthesis of 2-((*2E*, *6E*)-15-carboxy-15,15-difluoro-14-hydroxy-2,6,14-trimethyl-9,9-diphosphonopentadeca-2,6-dienylamino) benzoic acid (**16**). To a solution of compound **14** (0.45 mmol) in anhydrous CH_2Cl_2 at 0 °C were added 2,4,6-collidine (0.59 mL, 4.5 mmol) and TMSI (0.58 mL, 4.5 mmol), and the reaction mixture was allowed to warm to room temperature over a period of 2 h. Toluene was then added, and the volatiles were removed in vacuo to afford a white solid. This material was dissolved in aqueous LiOH (5 mL, 1 N) at room temperature. After 24 h, the mixture was lyophilized to afford a gray solid **16**. ^{1}H NMR (300 MHz, D_2O) δ 7.96–7.82 (m, 1H), 7.39–7.25 (t, 1H, J = 7.2 Hz), 6.75–6.51 (q, 2H, J = 7.0 Hz), 5.51–5.32 (m, 2H), 4.45–3.75 (m, 3H), 2.16–1.25 (m, 23H). ^{13}C NMR δ 176.8, 176.6, 150.5, 140.3, 135.2, 133.3, 132.3, 131.5, 128.6, 127.7, 120.8, 117.6, 114.4, 77.9, 51.3, 39.8, 28.7, 27.4, 27.2, 24.7, 16.4, 14.7, 13.5. MS (ESI): m/z 624 $(M+H)^+$. HRMS (m/z): Calcd for $(C_{26}H_{39}F_2NO_{11}P_2+H)^+$ 642.2039, found 642.2042.

2.4. Cell viability and fluorescence imaging assay

Cells were seeded in 96-well plates in serum-containing media, and allowed to attach for 24 h. The medium was then removed and replaced with serum-free medium containing 0.2% BSA with or without bisphosphonates at various concentrations. The cells were incubated for 72 h. Following incubation, the medium was removed, the cells were washed, and cell viability was measured by using the standard MTT assay.

3. Results and discussion

3.1. Organic syntheses of bisphosphonate derivatives

Compounds **15** and **16** were prepared as potential multifunctional enzyme inhibitors in mevalonate pathway, as shown in Scheme 1. Firstly, 5-chloro-2-pentanone, ethylene glycol and *p*-toluenesulfonic acid monohydrate were heated under reflux in toluene to give protected compound **4**. Tetraethyl ethylidene bisphosphonate **3** is a well know important intermediate [24], which can undergo efficient Michael addition reactions with various nucleophiles due to its electrophilic property. Then, tetraethyl ethenylidenbisphosphonate **3** was reacted with the corresponding organomagnesium reagent **5** (from compound **4**) to afford compound **6**. The reaction was run by the dropwise addition of a THF solution of organomagnesium reagent **5** to a stirred solution of compound **3** in THF under N_2 at −15 °C. Compound **10** was then prepared from the geraniol [25]. The geraniol was first converted to the corresponding acetate **7** by treatment with acetic anhydride in the presence of catalytic amount of $La(NO_3)_3 \cdot 6H_2O$. The resulting compound **7** was oxidized with selenium dioxide to give the aldehyde **8**. Treatment of the aldehyde with methyl anthranilate under reductive amination condition, followed with the removal of acetate group afforded compound **9**. The treatment of alcohol **9** with PBr_3 gave the corresponding bromide **10**[25]. The allylic bromide **10** was coupled with compound **6** to afford compound **11** in modest yield. The hydrolysis of **11** in 80% acetic acid at 65 °C provided the corresponding ketone **12**, which was then reacted with ethyl bromofluoroacetate and bromodifluoroacetate through Reformatsky reaction yielding corresponding compounds **13** and **14**, respectively. Finally, the corresponding fluorescently tagged bisphosphonate salts **15** and **16** were obtained using standard hydrolysis conditions by treatment with trimethylsilyl iodide, followed by a basic work-up procedure.

3.2. Inactivation studies of compounds 15 and 16 for enzymes MVK, PMK, MDD, and FPPS

Three ATP-dependent enzymes, MVK, PMK, and MDD, were assayed spectrophotometrically following a continuous enzyme-coupled assay

Please cite this article as: J. Gao, et al., Multi-target-directed design, syntheses, and characterization of fluorescent bisphosphonate derivatives as multifunctional enzyme inhibitors in mevalonate pathway, Biochim. Biophys. Acta (2013), http://dx.doi.org/10.1016/j.bbagen.2013.02.011

Table 1
IC_{50} values of compounds **15** and **16** for rat MVK, PMK, MDD, and FPPS.

Compound	IC_{50} (μM)			
	Rat MVK	Rat PMK	Rat MDD	Rat FPPS
15	3.4	5.9	1.9	0.035
16	2.7	4.2	0.8	0.029

method reported previously [26]. FPPS was assayed following our previously established method [20]. The inhibitory effects of bisphosphonate derivatives **15** and **16** on the activities of these four enzymes were studied by using Dixon plot [27], and the IC_{50} values were determined by a reciprocal plot of a series of remaining velocity versus corresponding inhibitor concentration, as shown in Table 1. Bisphosphonate derivatives **15** and **16** both exhibited good inhibitory activity simultaneously against rat MVK, PMK, MDD, and FPPS with their IC_{50} values at from nanomolar to micromolar range. The structural difference between these two compounds is that compound **16** has two fluorine substituents while compound **15** has only one fluorine substituent. Compound **16** showed slightly better activity than compound **15**.

Because active sites of these enzymes all have two distinct binding sites that specifically bind two kinds of substrates, we performed inhibition kinetic studies of each compound with varying concentrations of one substrate while fixing another substrate concentration. Our results showed that compound **16** is competitive with both substrates of the enzymes MVK, PMK, and MDD (with example of MDD as shown in Figs. 1 and 2), indicating that compound **16** can bind simultaneously to both substrate binding sites of these enzymes. Compound **16** is composed of a hydrophilic part (mevalonate) and a hydrophobic part (geranyl group), which is similar to that of the substrates for ATP-dependent enzymes (MVK, PMK, and MDD) and FPPS.

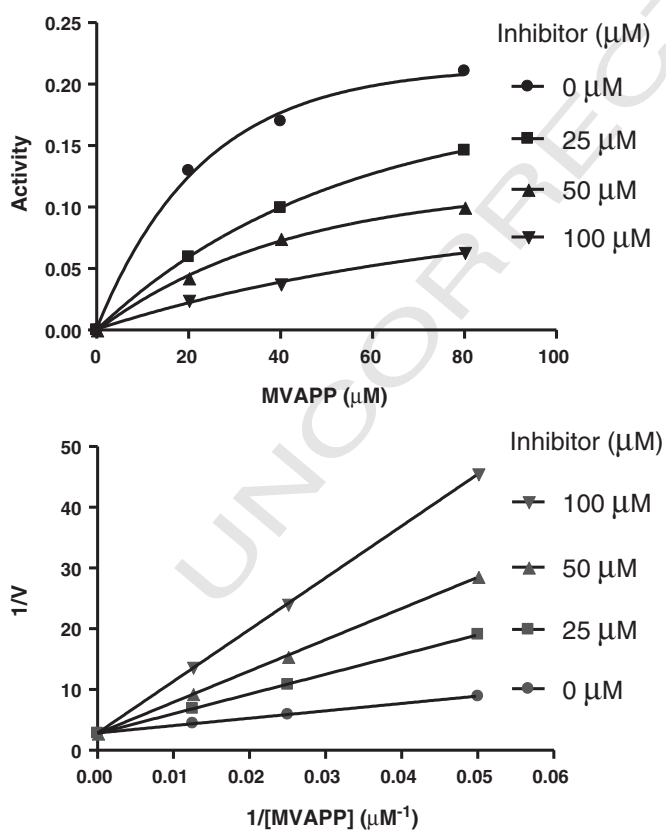

Fig. 1. Competitive inhibition of compound **16** against rat MDD with varying concentration of MVAPP. The concentration dependence of initial rates is shown in double-reciprocal plots, and was determined in the absence and presence of compound **16** at different concentrations.

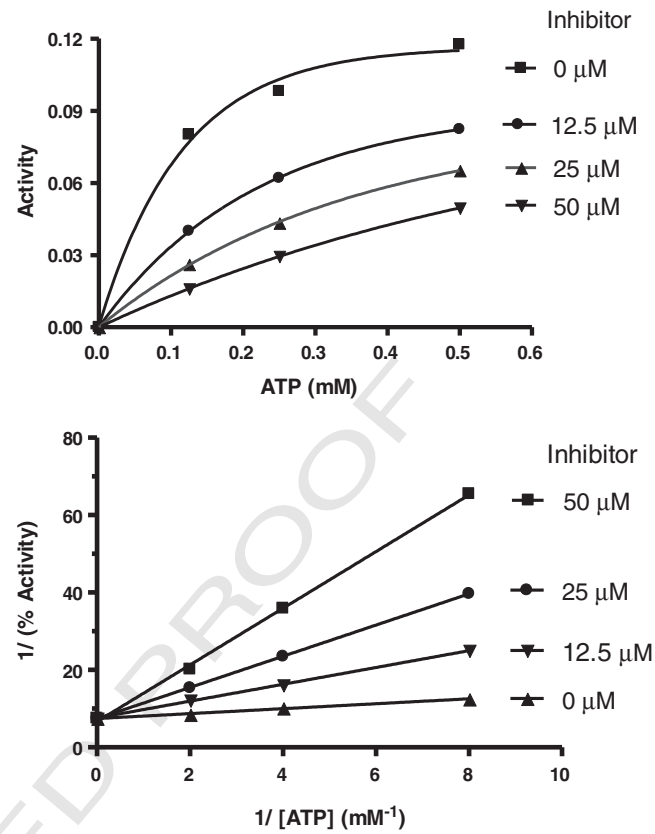

Fig. 2. Competitive inhibition of compound **16** against rat MDD with varying concentration of ATP. The concentration dependence of initial rates is shown in double-reciprocal plots, and was determined in the absence and presence of compound **16** at different concentrations.

This similarity of the property between the inhibitors and the substrates, together with their occupation of both binding sites, could all enhance their interactions with the enzymes, and therefore leading to good enzyme inhibitions.

3.3. Modeling studies on three-dimensional structure–activity relationship

In order to further study the binding modes of compounds **15** and **16** in the active sites of these four enzymes, we calculated the minimum energy conformations of compounds **15** and **16** docked into the models based on the crystal structures of rat MVK-ATP complex (PDB ID: 1KVK), human PMK (PDB ID: 3CH4), human MDD (PDB ID: 3D4J), and human FPPS–zoledronate–IPP complex (PDB ID: 2F8Z). MolDock scoring function was used to calculate score grids for rapid dock evaluation. Potential binding sites (cavities) were detected using the grid-based cavity prediction algorithm. The best docked interactive conformations of these two potent inhibitors in these four enzymes are shown in Fig. 3. The more active compound **16** gave lower total interactive energy and higher MolDock scores of −292.36, −136.21, −171.53 and −247.25 kcal/mol, respectively, indicating that compound **16** may has a higher binding affinity with residues in the active sites. Compounds **15** and **16** all bind to both ATP and mevalonate site of three ATP-dependent enzymes (MVK, PMK, and MDD). Molecular docking results are quite consistent with our enzyme kinetic analysis results. Compounds **15** and **16** also occupied both Zoledronic acid and IPP binding site in human FPPS X-ray crystal structure with Zoledronic acid inhibitor. Zoledronic acid is a bisphosphonate that has been developed for prevention and treatment of osteoporosis [28]. It has been reported that Zoledronic acid bind to FPPS through occupying DMAPP or GPP site of the enzyme [29]. Our results indicate that compounds **15** and **16** may occupy not only the GPP substrate binding

Please cite this article as: J. Gao, et al., Multi-target-directed design, syntheses, and characterization of fluorescent bisphosphonate derivatives as multifunctional enzyme inhibitors in mevalonate pathway, Biochim. Biophys. Acta (2013), http://dx.doi.org/10.1016/j.bbagen.2013.02.011

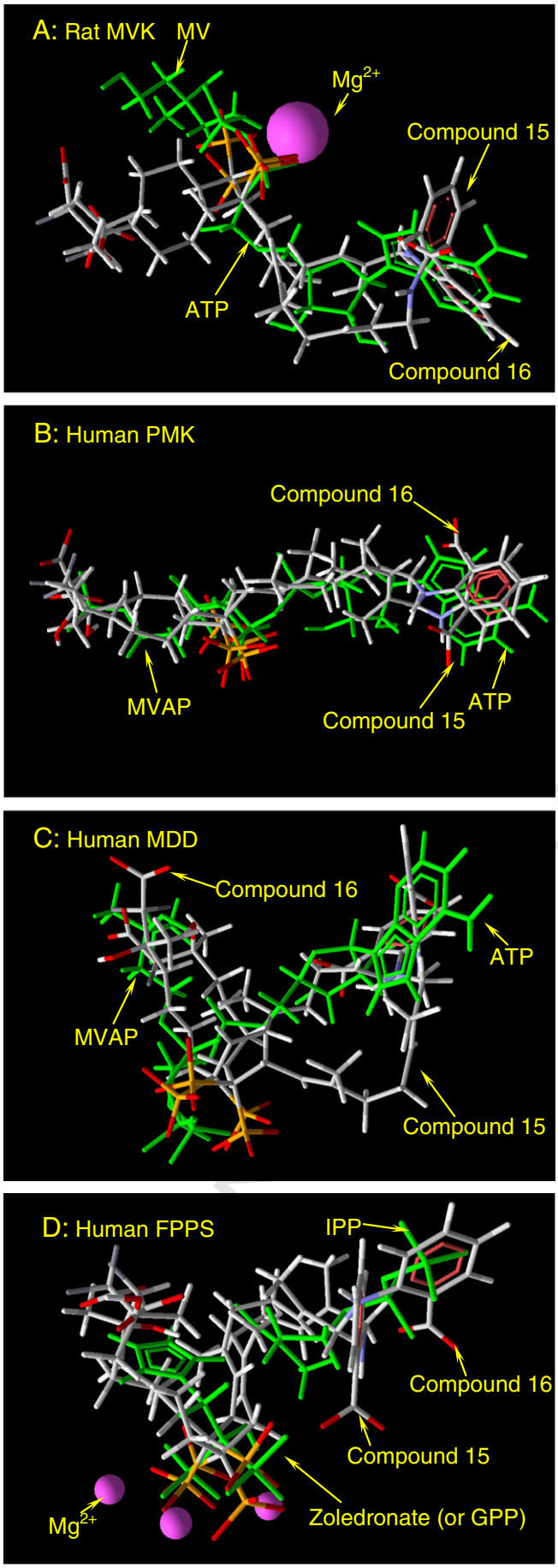

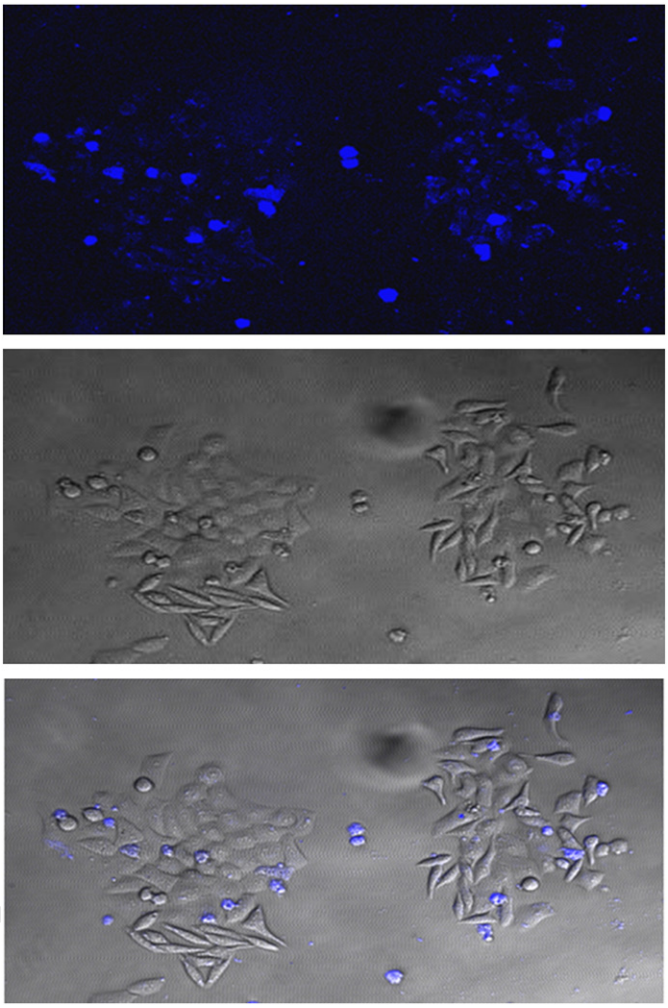

Fig. 4. Uptake of bisphosphonate analogue **15** by human Hela cells. Cells were incubated with compound **15** (1 μM) for 48 h, and were subsequently examined via fluorescent microscopy. Control cells under phase-contrast microscopy and under fluorescent microscopy are also shown.

site but also the IPP substrate binding site. The inhibitions of the enzymes are significantly enhanced by the binding of the inhibitors to both substrates binding sites of these four enzymes.

The detailed interactions, including hydrogen-bonding, hydrophobic and electrostatic interactions, between the inhibitors and the enzymes, were examined as shown in supporting information. Compounds **15** and **16** have similar structures, and therefore, similar enzyme-inhibitor interactions were observed. Our docking results indicated that these two compounds have good interactions with the enzyme active sites via hydrogen bonds, metal ions, hydrophobic interactions, and electrostatic interactions. Overall, hydrogen bonding and electrostatic interactions among the bisphosphonates, carboxylate, Mg^{2+}, hydroxyl group, and the side chains of amino acids help to hold the inhibitors in the active sites, and play important roles in

Fig. 3. The binding modes of compounds **15** and **16** to the models of crystal structure of rat MVK-ATP complex (PDB ID: 1KVK), human PMK (PDB ID: 3CH4), human MDD (PDB ID: 3D4J), and human FPPS–zoledronate–IPP complex (PDB ID: 2F8Z). MolDock scoring function was used to calculate score grids for rapid dock evaluation. Potential binding sites (cavities) were detected using the grid-based cavity prediction algorithm. Compounds **15** and **16** are represented as stick. The substrates ATP, MVA, MVAP, MVAPP, zoledronate or GPP, and IPP are represented in stick format (green). Mg^{2+} ions are represented in ball and stick format (pink). Crystal structure of the proteins without the substrate, and the positions of the corresponding substrates were predicted by using the MolDock software algorithm. Compounds **15** and **16** were found to fully overlap with two substrates of all these proteins.

Please cite this article as: J. Gao, et al., Multi-target-directed design, syntheses, and characterization of fluorescent bisphosphonate derivatives as multifunctional enzyme inhibitors in mevalonate pathway, Biochim. Biophys. Acta (2013), http://dx.doi.org/10.1016/j.bbagen.2013.02.011

the binding of the inhibitors with the enzymes. The geranyl group moiety shows strong hydrophobic interactions with nearby important amino acids, and the orientations of these amino acid side chains play important roles for enhancing the potency of the inhibitors.

3.4. Effects of blue bisphosphonate derivatives on cell viability and cell localization

Some previous studies have shown that bisphosphonates exert direct cytostatic and proapoptotic effects in the ranges of several to thousands micromolar on a variety of human tumor cell lines (myeloma, breast, prostate, pancreas) in a concentration- and time-dependent manner [30–33]. However, these bisphosphonates are rapidly adsorbed by bone, therefore, mainly used in treating bone-related diseases. So, it is desirable to have some relatively lipophilic bisphosphonates, which could be generally used as potential anticancer or antiparasitic agents [34]. In the present study, compounds **15** and **16** showed relatively good cell viability to Hela cells with their IC_{50} values of 32.8 ± 8.5 μM and 18.7 ± 3.1 μM, respectively, which could serve as lead compounds for further improvement. Compounds **15** and **16** are composed of some hydrophilic parts (carboxylate and bisphosphonate) and hydrophobic parts (geranyl group and benzene ring), which may facilitate their penetration of lipid membranes to reach the target enzymes, therefore increasing their effectiveness.

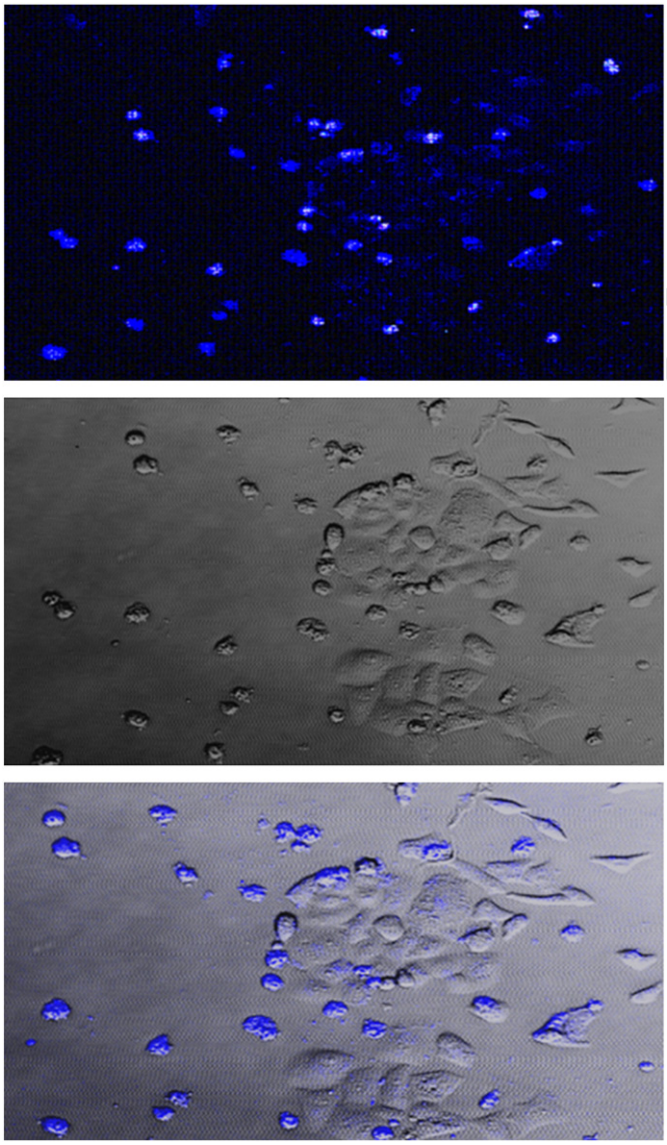

Fig. 5. Uptake of bisphosphonate analogue **16** by human Hela cells. Cells were incubated with compound **16** (1 μM) for 48 h, and were subsequently examined via fluorescent microscopy. Control cells under phase-contrast microscopy and under fluorescent microscopy are also shown.

It should be noted that compounds **15** and **16** are fluorescent due to their incorporation of an anthranilate fluorophore, which may be useful in studies of bisphosphonate localization both in cultured cells and in whole organisms. Fluorescence imaging is a very important technique for biological studies and clinical applications due to high temporal and spatial resolutions, and fluorescent bisphosphonates could be potentially used as biological probes. In the present study, fluorescent microscopy was performed to assess the cellular uptake of the fluorescent compounds **15** and **16**. Hela cells were incubated with compound **15** or **16** (1 μM) for 48 h, and were subsequently examined via confocal fluorescent microscopy. As shown in Figs. 4 and 5, the fluorescence microscopy clearly shows that fluorescent compounds **15** and **16** can easily penetrate Hela cells.

In summary, two multi-target-directed inhibitors **15** and **16** based on bisphosphonate were synthesized and evaluated against rat mevalonate kinase, phosphomevalonate kinase, mevalonate 5-diphosphate decarboxylase, and farnesyl pyrophosphate synthase. These two compounds showed good inhibition for all these enzymes in mevalonate pathway with high inhibitory activities. Multifunctional enzyme inhibitors are generally more effective than single enzyme inhibitors, with fewer side effects. The potential therapeutic applications of these multifunctional inhibitors could extend beyond the treatment of metastatic bone disease to encompass soft-tissue tumors and other diseases such as hypercholesteremia, in which targeting the mevalonate pathway has been shown to be effective. These results suggest a valuable role for such compounds as metabolic probes in cell cultures, and encourage further efforts to design bisphosphonate-based inhibitors.

Acknowledgements

We thank City University of Hong Kong and Sun Yat-sen University for financial support of this study.

Appendix A. Supplementary data

Cloning, expression, and purification of His-tagged rat phosphomevalonate kinase. The detailed interactions including hydrogen-bonding, hydrophobic and electrostatic interactions between the inhibitors and the enzymes in docking analysis. The above information can be found in the online version at http://dx.doi.org/10.1016/j.bbagen.2013.02.011.

References

[1] I. Buhaescu, H. Izzedine, Mevalonate pathway: a review of clinical and therapeutical implications, Clin. Biochem. 40 (2007) 575–584.
[2] W.A. Freed-Pastor, H. Mizuno, X. Zhao, A. Langerod, S.H. Moon, R. Rodriguez-Barrueco, A. Barsotti, A. Chicas, W.C. Li, A. Polotskaia, M.J. Bissell, T.F. Osborne, B. Tian, S.W. Lowe, J.M. Silva, A.L. Borresen-Dale, A.J. Levine, J. Bargonetti, C. Prives, Mutant p53 disrupts mammary tissue architecture via the mevalonate pathway, Cell 148 (2012) 244–258.
[3] K.M. Swanson, R.J. Hohl, Anti-cancer therapy: targeting the mevalonate pathway, Curr. Cancer Drug Targets 6 (2006) 15–37.
[4] E. Oldfield, Targeting isoprenoid biosynthesis for drug discovery: bench to bedside, Acc. Chem. Res. 43 (2010) 1216–1226.
[5] J.L. Goldstein, M.S. Brown, Regulation of the mevalonate pathway, Nature 343 (1990) 425.
[6] K.L. Kavanagh, K. Guo, J.E. Dunford, X. Wu, S. Knapp, F.H. Ebetino, M.J. Rogers, R.G.G. Russell, U. Oppermann, The molecular mechanism of nitrogen-containing bisphosphonates as antiosteoporosis drugs, Proc. Natl. Acad. Sci. 103 (2006) 7829–7834.
[7] A.J. Brown, Cholesterol, statins and cancer, Clin. Exp. Pharmacol. Physiol. 34 (2007) 135–141.
[8] Y.S. Lin, J. Park, J.W. De Schutter, X.F. Huang, A.M. Berghuis, M. Sebag, Y.S. Tsantrizos, Design and synthesis of active site inhibitors of the human farnesyl pyrophosphate synthase: apoptosis and inhibition of ERK phosphorylation in multiple myeloma cells, J. Med. Chem. 55 (2012) 3201–3215.

[9] Y. Qiao, J. Gao, Y. Qiu, L. Wu, F. Guo, K.K. Lo, D. Li, Design, synthesis, and characterization of piperazinedione-based dual protein inhibitors for both farnesyltransferase and geranylgeranyltransferase-I, Eur. J. Med. Chem. 46 (2011) 2264–2273.
[10] C. Bolego, R. Baetta, S. Bellosta, A. Corsini, R. Paoletti, Safety considerations for statins, Curr. Opin. Lipidol. 13 (2002) 637–644.
[11] J. Armitage, The safety of statins in clinical practice, Lancet 370 (2007) 1781–1790.
[12] S. Bellosta, R. Paoletti, A. Corsini, Safety of statins, Circulation 109 (2004) III-50–III-57.
[13] L.K. Bachrach, L.M. Ward, Clinical review: bisphosphonate use in childhood osteoporosis, J. Clin. Endocrinol. Metab. 94 (2009) 400–409.
[14] J. Brown, M. Zacharin, Safety and efficacy of intravenous zoledronic acid in paediatric osteoporosis, J. Pediatr. Endocrinol. Metab. 22 (2009) 55–64.
[15] J. Ichikawa, E. Sato, H. Haro, T. Ando, S. Maekawa, Y. Hamada, Successful treatment of SAPHO syndrome with an oral bisphosphonate, Rheumatol. Int. 29 (2009) 713–715.
[16] N.B. Watts, Treatment of osteoporosis with bisphosphonates, Endocrinol. Metab. Clin. 27 (1998) 419–439.
[17] F. Fulfaro, A. Casuccio, C. Ticozzi, C. Ripamonti, The role of bisphosphonates in the treatment of painful metastatic bone disease: a review of phase III trials, Pain 78 (1998) 157–169.
[18] M.A. Maalouf, A.J. Wiemer, C.H. Kuder, R.J. Hohl, D.F. Wiemer, Synthesis of fluorescently tagged isoprenoid bisphosphonates that inhibit protein geranylgeranylation, Bioorg. Med. Chem. 15 (2007) 1959–1966.
[19] A.P.C. Chen, Y.H. Chen, H.P. Liu, Y.C. Li, C.T. Chen, P.H. Liang, Synthesis and application of a fluorescent substrate analogue to study ligand interactions for undecaprenyl pyrophosphate synthase, J. Am. Chem. Soc. 124 (2002) 15217–15224.
[20] J. Gao, X. Chu, Y. Qiu, L. Wu, Y. Qiao, J. Wu, D. Li, Discovery of potent inhibitor for farnesyl pyrophosphate synthase in the mevalonate pathway, Chem. Commun. 46 (2010) 5340–5342.
[21] Y. Qiu, D. Li, Inhibition of mevalonate 5-diphosphate decarboxylase by fluorinated substrate analogs, Biochim. Biophys. Acta 1760 (2006) 1080–1087.
[22] D.L.X. Chu, Cloning, expression, and purification of His-tagged rat mevalonate kinase, Protein Expression Purif. 27 (2003) 165–170.
[23] A.E. Schulte, R. van der Heijden, R. Verpoorte, Microplate enzyme-coupled assays of mevalonate and phosphomevalonate kinase from *Catharanthus roseus* suspension cultured cells, Anal. Biochem. 269 (1999) 245–254.
[24] G. Bansal, J.E.I. Wright, C. Kucharski, H. Uludag, A dendritic tetra(bisphosphonic acid) for improved targeting of proteins to bone, Angew. Chem. Int. Ed. 44 (2005) 3710–3714.
[25] M.K. Kim, T.S. Kleckley, A.J. Wiemer, S.A. Holstein, R.J. Hohl, D.F. Wiemer, Synthesis and activity of fluorescent isoprenoid pyrophosphate analogues, J. Org. Chem. 69 (2004) 8186–8193.
[26] J. Eyzaguirre, D. Valdebenito, E. Cardemil, Pig liver phosphomevalonate kinase: kinetic mechanism, Arch. Biochem. Biophys. 454 (2006) 189–196.
[27] B.T. Burlingham, T.S. Widlanski, An intuitive look at the relationship of Ki and IC50: a more general use for the Dixon plot, J. Chem. Educ. 80 (2003) 214.
[28] A.J. Roelofs, K. Thompson, S. Gordon, M.J. Rogers, Molecular mechanisms of action of bisphosphonates: current status, Clin. Cancer Res. 12 (2006) 6222s–6230s.
[29] J.H. Mao, S. Mukherjee, Y. Zhang, R. Cao, J.M. Sanders, Y.C. Song, Y.H. Zhang, G.A. Meints, Y.G. Gao, D. Mukkamala, M.P. Hudock, E. Oldfield, Solid-state NMR, crystallographic, and computational investigation of bisphosphonates and farnesyl diphosphate synthase–bisphosphonate complexes, J. Am. Chem. Soc. 128 (2006) 14485–14497.
[30] J. Body, R. Bartl, P. Burckhardt, P. Delmas, I. Diel, H. Fleisch, J. Kanis, R. Kyle, G. Mundy, A. Paterson, Current use of bisphosphonates in oncology. International bone and cancer study group, J. Clin. Oncol. 16 (1998) 3890–3899.
[31] R. Coleman, Bisphosphonates in breast cancer, Ann. Oncol. 16 (2005) 687–695.
[32] J.R. Green, Antitumor effects of bisphosphonates, Cancer 97 (2003) 840–847.
[33] H. Neville-Webbe, I. Holen, R. Coleman, The anti-tumour activity of bisphosphonates, Cancer Treat. Rev. 28 (2002) 305–319.
[34] D. Mukkamala, J.H. No, L.M. Cass, T.K. Chang, E. Oldfield, Bisphosphonate inhibition of a plasmodium farnesyl diphosphate synthase and a general method for predicting cell-based activity from enzyme data, J. Med. Chem. 51 (2008) 7827–7833.

Please cite this article as: J. Gao, et al., Multi-target-directed design, syntheses, and characterization of fluorescent bisphosphonate derivatives as multifunctional enzyme inhibitors in mevalonate pathway, Biochim. Biophys. Acta (2013), http://dx.doi.org/10.1016/j.bbagen.2013.02.011